THE JOURNAL OF BIOLOGICAL CHEMISTRY VOL. 287, NO. 22, pp. 18218–18229, May 25, 2012

N-Glycosylation of TRPM8 Ion Channels Modulates Temperature Sensitivity of Cold Thermoreceptor Neurons*[S]

Received for publication, October 18, 2011, and in revised form, March 19, 2012 Published, JBC Papers in Press, April 5, 2012, DOI 10.1074/jbc.M111.312645

María Pertusa[‡§1], **Rodolfo Madrid**[‡§2], **Cruz Morenilla-Palao**[‡], **Carlos Belmonte**[‡], **and Félix Viana**[‡3]

From the [‡]*Instituto de Neurociencias de Alicante, Universidad Miguel Hernández-Consejo Superior de Investigaciones Científicas, 03550 Alicante, Spain and the* [§]*Departamento de Biología, Facultad de Química y Biología, Universidad de Santiago de Chile, Santiago 9160000, Chile*

Background: TRPM8 channel is *N*-glycosylated, a post-translational modification affecting trafficking and gating properties of other TRP channels.
Results: Preventing *N*-glycosylation reduces responses of TRPM8 to agonists (cold and menthol) due to a change in its biophysical properties.
Conclusion: *N*-Glycosylation is an important determinant of TRPM8 sensitivity to chemical and thermal stimuli.
Significance: *N*-Glycosylation of TRPM8 could play a modulatory role in cold thermoreceptor activity.

TRPM8 is a member of the transient receptor potential ion channel superfamily, which is expressed in sensory neurons and is activated by cold and cooling compounds, such as menthol. Activation of TRPM8 by agonists takes place through shifts in its voltage activation curve, allowing channel opening at physiological membrane potentials. Here, we studied the role of the *N*-glycosylation occurring at the pore loop of TRPM8 on the function of the channel. Using heterologous expression of recombinant channels in HEK293 cells we found that the unglycosylated TRPM8 mutant (N934Q) displays marked functional differences compared with the wild type channel. These differences include a shift in the threshold of temperature activation and a reduced response to menthol and cold stimuli. Biophysical analysis indicated that these modifications are due to a shift in the voltage dependence of TRPM8 activation toward more positive potentials. By using tunicamycin, a drug that prevents *N*-glycosylation of proteins, we also evaluated the effect of the *N*-glycosylation on the responses of trigeminal sensory neurons expressing TRPM8. These experiments showed that the lack of *N*-glycosylation affects the function of native TRPM8 ion channels in a similar way to heterologously expressed ones, causing an important shift of the temperature threshold of cold-sensitive thermoreceptor neurons. Altogether, these results indicate that post-translational modification of TRPM8 is an important mechanism modulating cold thermoreceptor function, explaining the marked differences in temperature sensitivity observed between recombinant and native TRPM8 ion channels.

Ambient temperature detection is a critical biological process carried out by specialized terminals of primary afferent sensory neurons in the dorsal root ganglia and trigeminal ganglia (TG)[4] (1). Thermosensitive nerve endings express a subset of proteins of the transient receptor potential (TRP) ion channel superfamily that is activated at different temperatures ranges, making these cationic ion channels key elements in the temperature sensing machinery of peripheral nerve endings (2, 3).

Among thermo-TRPs, TRPM8 (Transient Receptor Potential Melastatine 8) is a nonselective cation channel activated by mild cold temperatures and cooling compounds such as menthol, eucalyptol, and icilin (4, 5). Like several other TRP channels, TRPM8 is also gated by voltage (6–8). The voltage dependence of TRPM8 is characterized by a strong outward rectification at depolarized transmembrane potentials and a rapid and voltage-dependent closure at negative membrane potentials. Cooling and menthol application shift the activation curve of TRPM8 toward more negative potentials, increasing the probability of channel openings at physiological membrane potentials (7). These functional properties, its selective expression in a subset of small sensory neurons and behavioral findings in TRPM8 knock-out mice (9–11), indicate that TRPM8 is a key element in the molecular machinery transducing cold temperatures at sensory nerve endings.

In 2006, two groups reported independently that TRPM8 is *N*-glycosylated (*i.e.* modified by the covalent addition of a sugar moiety) in the extracellular loop between transmembrane domain five and six, specifically in a Asn residue at position 934, near the pore region (12, 13). These studies showed that the unglycosylated mutant displayed a reduction of TRPM8 levels at the cell surface, resulting in a smaller response to agonists. Both studies favored impairment in the traffic of channels to the plasma membrane as causal to the reduced activity. Related with the role of *N*-glycosylation in traffic, we have recently described that glycosylation at the Asn-934 residue also facilitates segregation of TRPM8 into membrane lipid rafts (14).

* This work was supported in part by Spanish MICIIN Projects SAF2010-14990 (to F. V.) and CONSOLIDER-INGENIO CSD2007-00023 (to C. B.).
[S] This article contains supplemental Figs. S1, "Methods," and additional references.
[1] Supported by a predoctoral fellowship from the Spanish Ministry of Education and Science and FONDECYT Grant 3110128.
[2] Supported by a postdoctoral fellowship of the Spanish Fundación Marcelino Botín and FONDECYT Grant 1100983.
[3] To whom correspondence should be addressed. Tel.: 34-965919347; Fax: 34-965919561; E-mail: felix.viana@umh.es.

[4] The abbreviations used are: TG, trigeminal ganglia; TRP, transient receptor potential; ER, endoplasmic reticulum; pF, picofarad.

Many ion channels are modified by the addition of carbohydrate residues, not only affecting their trafficking and targeting to specific compartments but also their gating (15–21). This regulated glycosylation is an additional modulatory mechanism of ion channels, increasing their functional diversity, like their phosphorylation state. Besides TRPM8, several other TRP channels are also known to undergo glycosylation, with important functional consequences (reviewed in Refs. 22–24). In TRPV5, a channel critical for Ca^{2+} reabsorption in the distal convoluted tubule of the kidney, cleavage of a single *N*-linked oligosaccharide by Klotho, a glucuronidase enzyme, stabilizes the channel at the apical plasma membrane (25). In TRPC6 and TRPC3, two closely related cation channels, differences in *N*-glycosylation pattern are responsible for their distinct functional properties, switching the channel from a receptor-regulated mode to a constitutively active mode (26). In TRPV4, an osmosensitive TRP channel, mutation of a single *N*-glycosylation site within the pore forming loop increases the expression of membrane-bound channels compared with wild type (27). Another example is TRPV1, which is also *N*-glycosylated at a position near the pore loop. This *N*-glycosylation affects the sensitivity of TRPV1 to capsaicin and capsazepine (28). These observations suggest that *N*-glycosylation of TRPM8 might affect its function by mechanisms other than, or in addition to, events involving traffic of the channel to the membrane.

Previous studies on TRPM8 glycosylation were performed exclusively on heterologous systems, with artificially high levels of expressed channels. Despite their intrinsic interest, these findings may not apply to a more physiological context. For example, we have found important differences in the gating properties of native and recombinant TRPM8 channels, leading to dramatic changes in voltage sensitivity and apparent thermal threshold (8). Moreover, others have reported differences in the glycosylation status of heterologously expressed and native TRPV1 channels (24). Thus, we thought it was important to evaluate the functional role of TRPM8 *N*-glycosylation in native cold receptors. Indeed, we could observe an important contribution of this post-translational modification to the gating properties of the channel in neurons, suggesting that *N*-glycosylation could represent an important modulatory factor of cold thermoreceptor activity.

EXPERIMENTAL PROCEDURES

Molecular Biology and Site-directed Mutagenesis—The full-length cDNA encoding mouse TRPM8 (NM_134252) in pcDNA5 (Invitrogen) was kindly provided by Dr. Ardem Patapoutian (Scripps Research Institute, La Jolla, CA). The TRPM8 mutants were obtained by site-directed mutagenesis using *Pfu* Turbo (Stratagene), with the following primers: N934Q forward 5′-CTTCTCGGGACAAGAGTCCAAGC-3′ and reverse 5′-GCTTGGACTCTTGTCCCGAGAAG-3′; N934D forward 5′-CCTTCTCGGGAGATGAGTCCAAGCC-3′ and reverse 5′-GGCTTGGACTCATCTCCCGAGAAGG-3′; and N934K, forward 5′-CCTTCTCGGGAAAAGAGTCCAAGCC-3′ and reverse 5′-GGCTTGGACTCTTTTCCCGAGAAGG-3′.

Western Blot—HEK293 cells transiently transfected with wild type or mutant TRPM8 channels and trigeminal ganglia cultured cells were washed with phosphate-buffered saline and solubilized in radioimmune precipitation assay buffer (phosphate-buffered saline, pH 7.4, 0.1% (w/v) SDS, 1% (v/v) Nonidet P-40, 0.5% (w/v) sodium deoxycholate) supplemented with a protease inhibitor mixture (Roche Applied Science). Lysates were centrifuged at 10,500 × *g* for 15 min at 4 °C, and the protein concentration was measured in the supernatant by using BCA protein assay reagent. Equal amounts of protein for each condition (15–30 μg) were denatured at 95 °C for 5 min, loaded onto a 7.5% SDS-polyacrylamide gel, and electrophoresed. Proteins were transferred to a nitrocellulose membrane, blocked with 10% skim milk in TBS, and incubated with antibodies against mouse TRPM8 (diluted 1:500) (14). Horseradish peroxidase (HRP)-coupled anti-rabbit secondary antibodies (Sigma) were used at a final concentration of 1:2000 for detection, and the signal was developed with an enhanced chemiluminescence kit (Amersham Biosciences) and recorded by using an image analyzer LAS-1000Plus (Fujifilm).

Cell Surface Biotinylation—Biotinylation assays were performed using the Pierce cell surface protein isolation kit (Thermo Scientific). Briefly, 48 h post-transfection, 10^6 HEK293 cells were washed twice with ice-cold phosphate-buffered saline (PBS), pH 7.2, and incubated with 0.25 mg/ml of sulfo-NHS-SS-biotin in PBS for 30 min at 4 °C. After quenching free biotin, biotinylated cells were lysed in 200 μl of lysis buffer with protease inhibitor mixture (Roche Applied Science). Cell lysates were sonicated, incubated for 30 min on ice, and finally harvested at 10,500 × *g* for 15 min at 4 °C. For each experimental condition, the same amounts of protein (100–150 μg) were incubated with 90 μl of NeutrAvidin beads for 3 h at room temperature, after collecting a small aliquot as input control. Beads were washed three times with lysis buffer, and proteins were eluted with SDS sample buffer (62.5 mM Tris-HCl, pH 6.8, 1% SDS, 10% glycerol, and 50 mM DTT) for immunoblot analysis. Quantification analysis was performed with ImageGauge Version 4.0 software (Fujifilm).

Cell Culture, Transfection, and Mouse Trigeminal Neurons Culture—3×10^5 HEK293 cells were plated in 24-well dishes and transiently transfected with 2 μg of the indicated DNA and Lipofectamine 2000 (Invitrogen), following the manufacturer's indications. At 48 h post-transfection, protein expression analysis and calcium imaging experiments were performed. Trigeminal ganglion neurons from neonatal mice were cultured as described previously (29). Briefly, the trigeminal ganglia were isolated and disaggregated in 1 mg/ml collagenase type 1A and cultured in Dulbecco's modified Eagle's medium/F-12 medium, containing 10% fetal bovine serum (Invitrogen), and supplemented with 4 mM L-glutamine (Invitrogen), 17 mM glucose, nerve growth factor (mouse 7 S, 100 ng/ml; Sigma), and antibiotics. Cells were plated on polylysine-coated glass coverslips and used during the following 48 h. All of the procedures involving animals were performed following European Union guidelines.

To inhibit the addition of *N*-linked sugars, transiently transfected HEK293 cells and trigeminal cultured neurons were grown in the presence of 5 μg/ml tunicamycin (Sigma) for 48 h. To suppress the transport of proteins from endoplasmic reticulum (ER) to the Golgi apparatus, cells were treated with 5 μg/ml brefeldin A (Sigma) for 20 h. Stocks of tunicamycin and

brefeldin A were prepared in ethanol at 5 and 1 mg/ml, respectively. The vehicle was added to the control (*i.e.* untreated) cells.

Fluorescence Ca^{2+} Imaging—The cells were loaded with 5 μM Fura-2 AM (Invitrogen) in standard extracellular solution (in mM) as follows: 140 NaCl, 3 KCl, 1.3 $MgCl_2$, 2.4 $CaCl_2$, 10 glucose, and 10 HEPES, pH 7.4, adjusted with NaOH, 297 mosM/kg, and supplemented with 0.02% Pluronic (Invitrogen) for 45 min at 37 °C in darkness. In the zero-calcium experiments, the solution contained (in mM) the following: 140 NaCl, 3 KCl, 1.3 $MgCl_2$, 1 EGTA, 10 glucose, 10 HEPES, pH 7.4, adjusted with NaOH. Fluorescence measurements were made by using a Leica DMIRE2 inverted microscope fitted with a 12-bit cooled CCD camera (Imago QE Sensicam; T.I.L.L. Photonics, Graefelfing, Germany). Fura-2 was excited at 340 and 380 nm with a Polychrome IV monochromator (T.I.L.L. Photonics), and the emitted fluorescence was filtered with a 510-nm long pass filter. Calibrated ratios (0.5 Hz) were displayed on-line with T.I.L.L. Vision software version 4.01 (T.I.L.L. Photonics). Bath temperature was sampled simultaneously (see below), and threshold temperature values for $[Ca^{2+}]_i$ elevation were estimated by linearly interpolating the temperature at the midpoint between the last base-line point and the first point at which a rise in $[Ca^{2+}]_i$ deviated by at least four times the S.D. of the base line.

Electrophysiological Recordings—Whole-cell voltage clamp recordings were performed simultaneously with temperature recordings. Standard patch pipettes (3–5 megohms) were made of borosilicate glass capillaries (Harvard Apparatus Ltd.) and contained (in mM): 140 CsCl, 0.6 $MgCl_2$, 1 EGTA, 10 HEPES, 1 $ATPNa_2$, and 0.1 GTPNa, pH adjusted to 7.4 with CsOH (278 mosM/kg). The bath solution was the same as in the calcium imaging experiments. Current signals were recorded with an Axopatch 200B patch clamp amplifier (Molecular Devices). Stimulus delivery and data acquisition were performed using pCLAMP9 software (Molecular Devices).

To estimate the shifts in the voltage dependence of activation of TRPM8 in HEK293 cells, current-voltage (*I-V*) relationships obtained from repetitive (0.2 Hz) voltage ramps (−100 to +150 or 180 mV, with a slope of 200 mV/s) were fitted with a function that combines a linear conductance multiplied by a Boltzmann activation term (56) as shown in Equation 1,

$$I = g \times (V - E_{rev})/(1 + \exp((V_{1/2} - V)/s)) \qquad \text{(Eq. 1)}$$

where g is the whole-cell conductance; E_{rev} is the reversal potential of the current; $V_{1/2}$ is the potential for half-maximal activation, and s is the slope factor. The assumption of a linear conductance is based on the observation by Voets *et al.* (7) that open TRPM8 channels exhibit ohmic *I-V* dependence. For each cell, fitting was started by analyzing a condition with strong channel activation, typically 100 μM menthol at 20 °C. The value obtained for the parameter g at this condition was defined as g_{max} and was used as a limit in the fitting of the remaining experimental conditions, $g < g_{max}$. E_{rev} was fixed at a value close to the measured reversal potential of the current evoked by menthol and cooling.

Temperature Stimulation—Coverslips with cultured cells were placed in a microchamber and continuously perfused with solutions warmed to ~34 °C. The temperature was adjusted with a water-cooled Peltier device placed at the inlet of the chamber and controlled by a feedback device. Cold sensitivity was investigated with a temperature drop from 34 to 15–18 °C. Temperature decreased and recovered in a quasi-exponential manner with a time constant of ~10 s.

RESULTS

TRPM8 Is an N-Glycosylated Protein—Previously, it has been reported that TRPM8 is an *N*-glycosylated protein in recombinant expression systems (12, 13). Studies in dorsal root ganglia neurons also confirmed that endogenous TRPM8 channels are highly glycosylated *in vivo* (14). To further study the *N*-glycosylation of TRPM8 in a native context, we cultured TG neurons that express TRPM8 endogenously and analyzed their immunoreactive profile to TRPM8. Both TRPM8 channels expressed in HEK293 cells and native channels from TG neurons show a band in Western blot larger than the size predicted from the cDNA sequence (128 kDa), consistent with the existence of post-translational modifications (Fig. 1*A*).

To study the effect of *N*-glycosylation on functional properties of TRPM8 channels, we used two different approaches. First, we employed drugs that eliminate the *N*-glycosylation. To this end, we used tunicamycin, an antibiotic that blocks the addition of carbohydrate molecules to asparagine residues of potential glycoproteins (30), and brefeldin A, which inhibits transport of proteins from the ER to Golgi complex and leads to protein accumulation inside the ER (31). In a second strategy, we used single point mutation of the asparagine 934, the only residue in TRPM8 where the *N*-glycosylation takes place (12–14), to a glutamine residue. In both strategies, the tunicamycin treatment and the point mutation of N934Q resulted in the detection of a single band of ~128 kDa, corroborating that TRPM8 is *N*-glycosylated in both recombinant and native systems (Fig. 1, *B* and *C*). Analysis of the glycosylation pattern of TRPM8 in transfected HEK293 cells revealed that a 48-h treatment with tunicamycin was the minimum time required to remove all *N*-glycosylated forms presents in the extract (Fig. 1*D*). In Fig. 1*E*, protein extract from TRPM8 expressed in HEK293 cells show three distinguishable bands, corresponding to different maturation states of TRPM8. After treatment with brefeldin A, the higher molecular weight band was eliminated. However, only the smaller band remained after tunicamycin treatment (Fig. 1, *B* and *D*). Taken together, our results suggest that the lower band represents the nonglycosylated channel, the intermediate band corresponds to the early *N*-glycosylated form produced in the ER, which results from the transfer of a mannose-rich precursor to the protein, and the higher molecular weight band represents the more mature *N*-glycosylation form, which is generated during their transit through the Golgi complex (32).

Effect of N-Glycosylation on TRPM8 Channel Function—To gain further insight into the role of *N*-glycosylation on TRPM8 channel function, we used calcium imaging techniques to compare the responses of HEK293 cells expressing TRPM8-WT and TRPM8-N934Q mutants to thermal and chemical stimuli. The protocol consisted of a cold temperature pulse from 34 to 20 °C, followed by a menthol stimulus at 34 °C, and a second

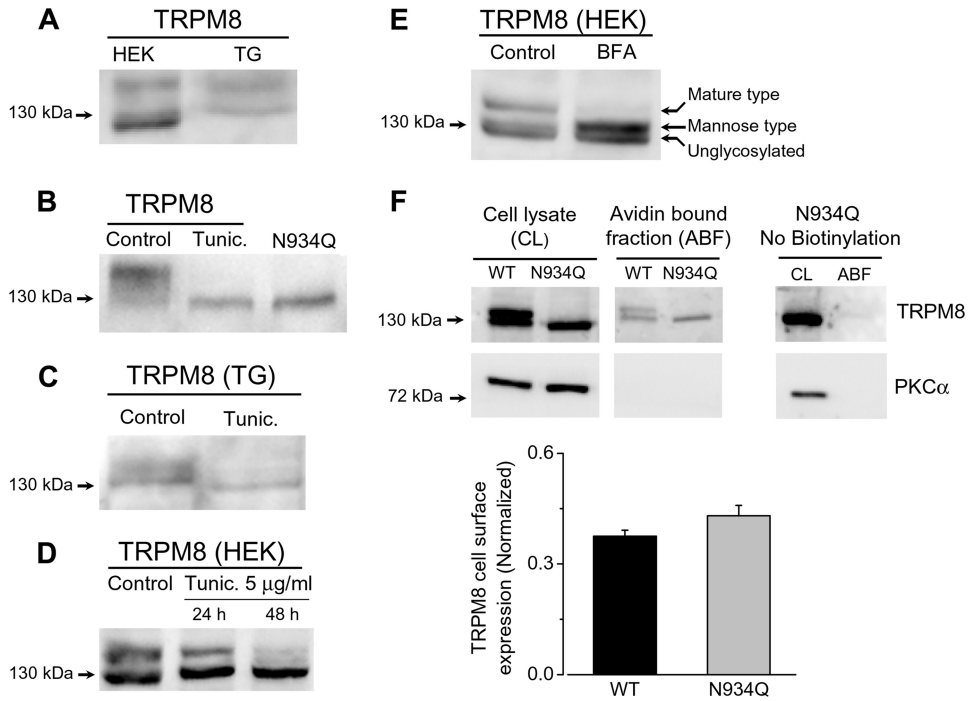

FIGURE 1. **Expression of *N*-glycosylated forms of recombinant and native TRPM8 channels.** *A,* Western blots of cell lysates from TRPM8-transfected HEK293 cells (*HEK*) and mouse TG neurons probed with an anti-TRPM8 antibody. *B,* non-*N*-glycosylated TRPM8-N934Q mutant and the wild type TRPM8 channel from tunicamycin-treated cells migrates faster than wild type channels. *C,* TRPM8 expression in trigeminal ganglia in control condition and 48 h after treatment with tunicamycin. *D,* time course of treatment with tunicamycin (*Tunic.*) (5 μg/ml) at 24 and 48 h. *E,* effect of treatment with brefeldin A (*BFA*) (5 μg/ml) for 20 h. TRPM8 protein was detected by an anti-TRPM8 antibody (1:500). *F,* representative Western blots from biotinylation assays using HEK293 cells transfected with the TRPM8-WT and the TRPM8-N934Q mutant. Biotinylated proteins were precipitated with Neutravidin beads (avidin-bound fraction, ABF) from cell lysates (*CL*) to measure the surface expression of TRPM8. Total expression of the ion channel was assessed by directly immunoblotting 15 μg of each cell lysate. The *left panel* corresponds to transfected HEK293 cells with TRPM8-N934Q mutant that were not subjected to cell surface biotinylation (*No biotinylation*). PKC-α was used as a control for cell membrane integrity. The normalized TRPM8 cell surface expression was calculated by expressing the intensities of the TRPM8 bands in the avidin-bound fraction as a fraction of those in the corresponding cell lysates. The *lower panel* shows TRPM8 cell surface expression, normalized to total TRPM8 expression. Data are means ± S.E. of three experiments from different batches of transfected cells. The two mean values did not differ from each other at the $p = 0.05$ level (Student's *t* test).

pulse of cold in the presence of menthol, which corresponds to a saturating stimulus (Fig. 2*A*) (4). Responses to cold or menthol in the TRPM8-N934Q mutant were strongly reduced as follows: for a cold stimulus, the increment in $[Ca^{2+}]_i$ was 378 ± 19 nM in TRPM8-WT ($n = 56$) and 93 ± 15 nM in the TRPM8-N934Q mutant ($n = 54$) ($p < 0.001$). In the same cells, $[Ca^{2+}]_i$ responses to 100 μM menthol were 234 ± 18 nM in TRPM8-WT and 98 ± 14 nM in TRPM8-N934Q ($p < 0.001$). In contrast, the amplitude of the $[Ca^{2+}]_i$ response to the saturating stimulus (*i.e.* menthol + cold) is the same in TRPM8-N934Q compared with TRPM8-WT (580 ± 19 nM *versus* 524 ± 26 nM; $p > 0.05$) (Fig. 2*B*). To rule out an effect of amino acid substitution in the TRPM8-N934Q mutant channel phenotype, HEK293 cells were transiently transfected with TRPM8-WT and treated thereafter for 48 h with tunicamycin. The results of the tunicamycin treatment were nearly identical to those obtained with the N934Q mutant channels. In tunicamycin-treated cells, responses to cold or menthol were strongly reduced, compared with control untreated cells (Fig. 2, *C* and *D*). These results confirm prior findings, which show that the N934Q mutation reduces the amplitude of TRPM8-dependent signals (12, 13). Previous reports suggested that this reduction could be the result of lower expression levels of the mutant channel at the plasma membrane (12, 13). In contrast, our biotinylation experiments show that expression levels of the TRPM8-N934Q mutant at the cell surface were similar to those observed with the wild type channel (Fig. 1*F*). Thus, we hypothesized that the reduction in the response could be due to a decrease in the sensitivity of the TRPM8-N934Q mutant to agonists, rather than secondary to a trafficking problem. To corroborate the data obtained with the biotinylation assay and to take advantage that TRPM8 can form functional channels within the ER (33, 34), we next tested the potential contribution of the intracellular pool of channels on TRPM8 responses. To study the functional response of TRPM8 channels exclusively present in the ER, we used the same stimulation protocol described above but in the absence of extracellular Ca^{2+}. Under this condition, only a strong stimulus (*i.e.* menthol plus cold) was able to evoke $[Ca^{2+}]_i$ responses from TRPM8-expressing cells (Fig. 2*A*). Moreover, responses to both agonists in zero Ca^{2+} (*i.e.* originating in the ER) were strongly reduced in the N934Q mutant ($p < 0.001$) and tunicamycin-treated cells ($p < 0.01$), compared with wild type (Fig. 2, *B* and *D*). If the absence of *N*-glycosylation causes the accumulation of the channels in the ER due to a trafficking defect, one would expect that responses in zero Ca^{2+} would be greater in the mutant compared with the wild type channel. In contrast, we observed a smaller response to the saturating stimulus in the mutant compared with the wild type channel. In the ER, the wild type TRPM8 channels present an immature *N*-glycosylation, whereas the TRPM8-N934Q mutant and the wild type channels in tunicamycin-treated cells are fully unglycosylated. The reduction in the response dis-

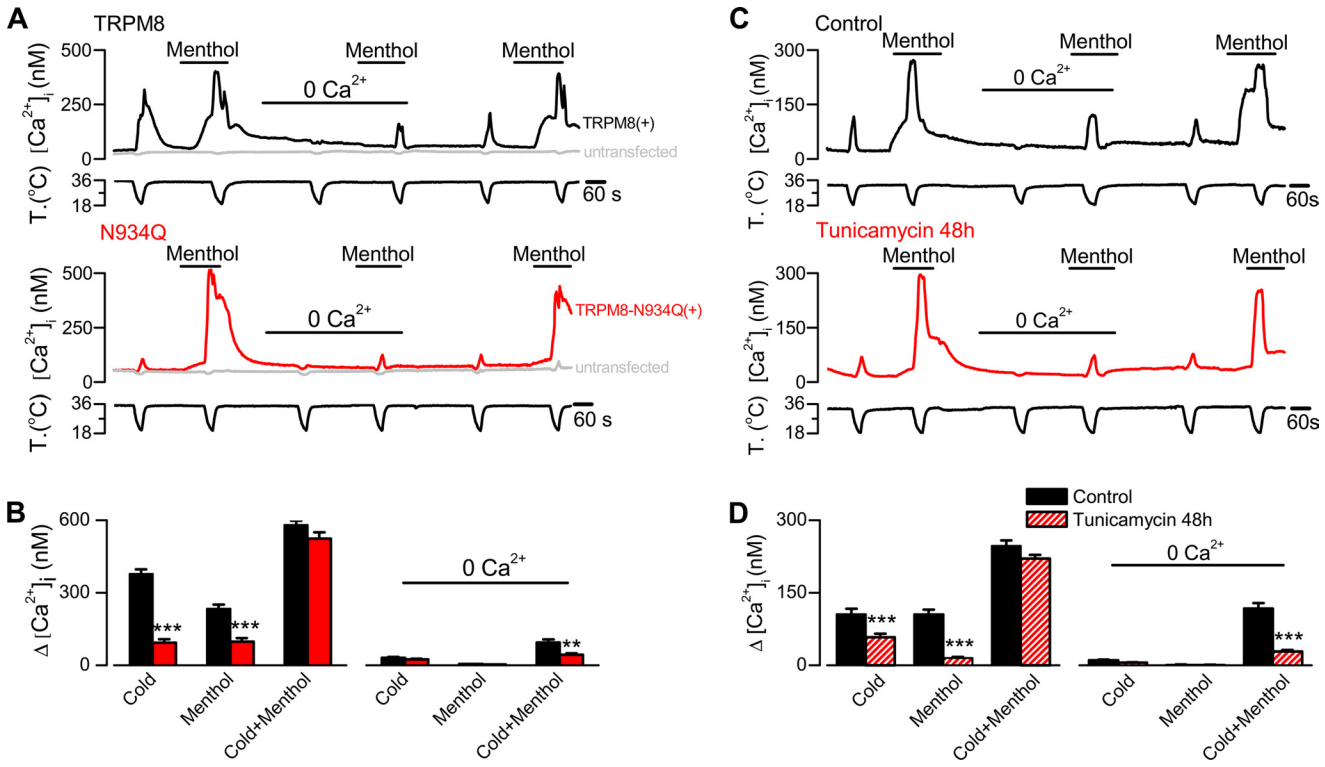

FIGURE 2. **Responses to cold and menthol are reduced in the nonglycosylated TRPM8 mutant.** *A,* representative intracellular calcium imaging traces showing responses to cold and 100 μM menthol in nontransfected HEK293 cells (*gray*) and cells expressing TRPM8-WT (*black*) or TRPM8-N934Q (*red*). The protocol was performed under normal (2.4 mM) and zero external Ca^{2+} conditions. Note the lack of response to cold or menthol in untransfected cells. *B,* summary histogram of the results obtained for the experimental protocol shown in *A*. Intracellular calcium increases for TRPM8-WT and TRPM8-N934Q were compared using an unpaired Student *t* test: ***, $p < 0.001$; TRPM8-WT, $n = 56$; TRPM8-N934Q, $n = 54$. *C,* representative traces showing intracellular calcium elevations to cold and 100 μM menthol in HEK293 cells expressing TRPM8-WT (*black*) in control and after 48 h of exposure to 5 μg/ml tunicamycin (*red*). The stimulation protocol was carried out with and without external Ca^{2+}. *D,* summary histogram of the results obtained with the experimental protocol shown in *C*. Intracellular calcium elevations in control and tunicamycin-treated cells were compared using an unpaired Student's *t* test: **, $p < 0.01$; ***, $p < 0.001$; control, $n = 81$; tunicamycin-treated, $n = 83$.

played by the mutant suggests that an immature *N*-glycosylation could also affect, in some degree, the activity of TRPM8 in the ER. Collectively, the results of biotinylation experiments, the very similar responses to saturating stimuli and the lack of evidence for a significant retention within the ER, strongly suggest that *N*-glycosylation affects primarily the sensitivity of TRPM8 channels to agonists.

Sensitivity of TRPM8 to Agonists Depends on N-Glycosylation—To further characterize the agonist sensitivity of the nonglycosylated channels, we examined their temperature threshold and their dose response to menthol. Although the calcium imaging method provides only an indirect estimate of channel activity, the apparent thermal threshold and the EC_{50} to menthol should not diverge significantly between TRPM8-WT and TRPM8-N934Q channels, if these differences are due primarily to lower expression levels of nonglycosylated channels within the plasma membrane. The dose-response curve shows that wild type channels are more sensitive to menthol than the N934Q mutant. The calculated menthol EC_{50} is 70 ± 8 μM for the wild type channel and 176 ± 13 μM for the N934Q mutant (Fig. 3*B*). In addition, the temperature threshold analysis (see "Experimental Procedures") allowed us to compare the sensitivity to thermal stimuli of these channels. In Fig. 3*C*, we represented the cumulative population of cells recruited by lowering temperature. The curve for TRPM8-N934Q mutant shows a significant shift toward lower temperatures, indicating that nonglycosylated TRPM8 channels are less sensitive to cold. The mean temperature threshold of the recombinant TRPM8 channel is around 26.5 °C, whereas in cells expressing the mutant TRPM8-N934Q channel, this value shifts to 24.0 °C ($p < 0.001$) (Fig. 3*D*). In conclusion, the lack of *N*-glycosylation changes the functional properties of TRPM8 channels, causing a loss of sensitivity to both physical and chemical agonists.

N-Glycosylation Affects Gating Properties of TRPM8—To further characterize the mechanism that could explain the differences in activity between glycosylated and nonglycosylated TRPM8 channels, we performed electrophysiological experiments. The protocol that we used for this approach is shown in Fig. 4*A*. The cells were held at −60 mV and presented with the three stimuli in sequence (cold, menthol, and cold in the presence of menthol). Voltage ramps from −100 to +180 mV were applied to generate *I-V* relationships in four conditions (control at 35 °C, cold, menthol, and cold plus menthol). Similar to calcium imaging experiments, HEK293 cells transfected with N934Q mutant displayed a marked decrease in the amplitude of the response to both cold and menthol stimuli (I_{cold} 0.1 ± 0.2 pA/pF; $I_{menthol}$ −3.4. ± 1.0 pA/pF) compared with cells transfected with the wild type channel (I_{cold} −3.9 ± 1.6 pA/pF; $I_{menthol}$ −17.7 ± 5.9 pA/pF) (Fig. 4*C*).

The gating of TRPM8 ion channels is voltage-dependent (6, 7). To estimate the maximal conductance (g_{max}), slope factor (s), and the voltage at 50% activation ($V_{½}$), the currents derived from the voltage ramps were fitted with a Boltzmann-linear

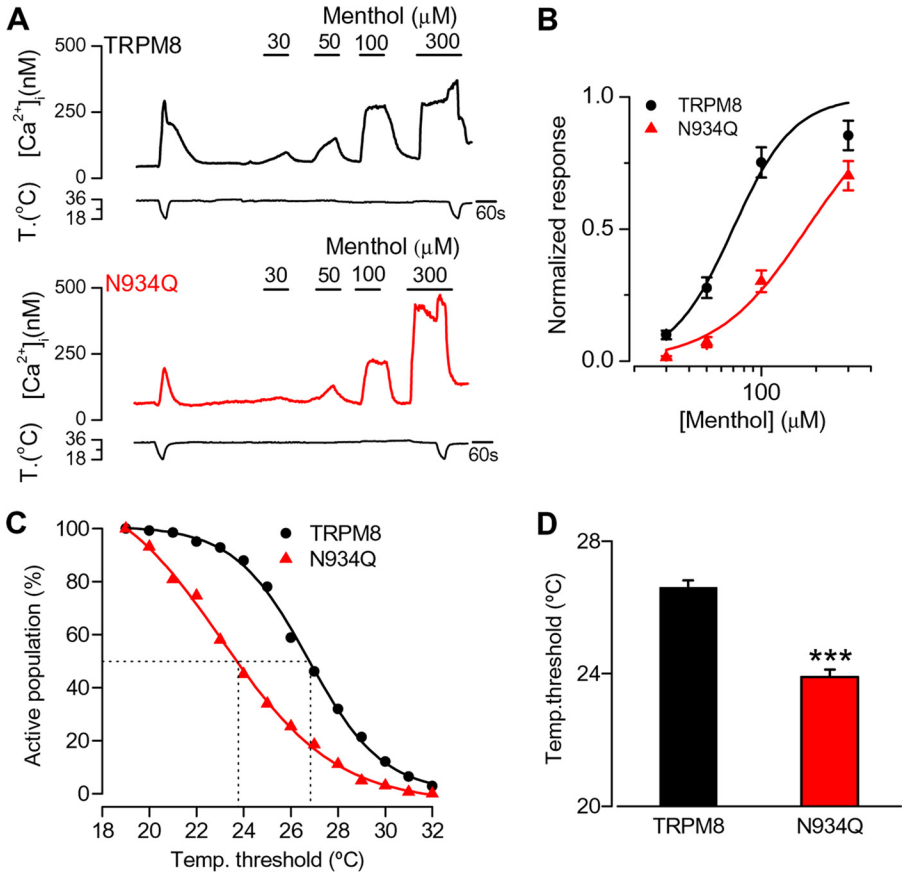

FIGURE 3. **Sensitivity of TRPM8 channels to agonists depends on the *N*-glycosylation.** *A,* time course of $[Ca^{2+}]_i$ response in transfected HEK293 cell with TRPM8-WT (*black*) and TRPM8 N934Q (*red*) during cooling ramps and applications of menthol at different concentrations. *B,* dose-response curves of responses to menthol in transfected HEK293 cells. The *solid lines* represent a fit to the Hill equation that yielded an EC_{50} of 70 ± 8 μM for TRPM8-WT and 176 ± 13 μM for TRPM8-N934Q (TRPM8-WT, $n = 29$; TRPM8-N934Q, $n = 14$). Responses were normalized to the amplitude obtained with maximal stimulation (menthol plus cold). *C,* percentage of active population recruited during a cooling ramp in HEK293 cells transfected with TRPM8-WT *versus* TRPM8-N934Q. *D, histogram* of temperature thresholds exhibited by HEK293 cells transfected with TRPM8-WT ($n = 141$) or TRPM8-N934Q ($n = 162$). Temperature thresholds were compared using a two-tailed unpaired Student's *t* test: ***, $p < 0.001$.

function (see under "Experimental Procedures"). The lack of *N*-glycosylation produced a clear shift in the $V_{½}$ of activation to more positive potentials (Fig. 4*D*), with no change in maximal conductance (Fig. 4*E*) and slope factor (Table 1), suggesting that decreased sensitivity to agonist displayed by the N934Q mutant is due primarily to an effect on the gating mechanism.

To further support these observations, we also estimated the expression level of both TRPM8-WT and TRPM8-N934Q channels in the plasma membrane, using nonstationary noise analysis (supplemental Fig. 1) (35). The estimated number of active channels per cell in both conditions was very similar (680 ± 98 channels for the wild type, $n = 7$, *versus* 471 ± 122, $n = 9$, for the N934Q mutant, $n = 9$; $p = 0.22$), corroborating the idea that the expression level of these channels are not significantly different. Unitary conductance, estimated from the mean single channel unitary current for the wild type and mutant channel at 19 °C, was ~60 picosiemens in both cases, similar to the values reported previously for TRPM8 wild type channels (6).

Contribution of Negative Charge at Position 934 on TRPM8 Channel Activity—Previously, we reported that mature *N*-glycosylation of TRPM8 contains terminal sialic acid residues, which are negatively charged (14). This post-translational modification is located at a residue in the vicinity of the pore region. Thus, we considered the possibility that removal of the negative charge provided by the *N*-glycosylation could explain the altered function in the N934Q mutant. To test this hypothesis, we performed different point mutations at position 934. In one mutant (N934K), the original asparagine was replaced by lysine, a positively charged amino acid. In the mutant N934D, this residue was replaced by an aspartic acid, a negatively charged amino acid. As shown in Fig. 5*A*, replacing the asparagine with a negatively charged residue partially recovers the response amplitude to cold temperature, compared with the neutral N934Q mutant and the positively charged N934K mutant. The increase in the responses to cold of the N934D mutant is not accompanied by a significant change in temperature activation threshold, compared with the other two mutations (Fig. 5*B*). The response of the N934Q and N934K mutants to a saturating stimulus (cold plus menthol) also shows a slight decrease compared with the wild type channel, which is not seen in the N934D mutant (Fig. 5*C*). Also, as shown in Fig. 5*D*, the EC_{50} value to menthol in N934D mutant is lower than in the mutants N934K and N934Q.

N-Glycosylation of TRPM8 Has an Important Role in Tuning Temperature Threshold of Cold Thermoreceptor Neurons—To determine the influence of TRPM8 *N*-glycosylation in a more physiological context, we studied the responses in cold-sensi-

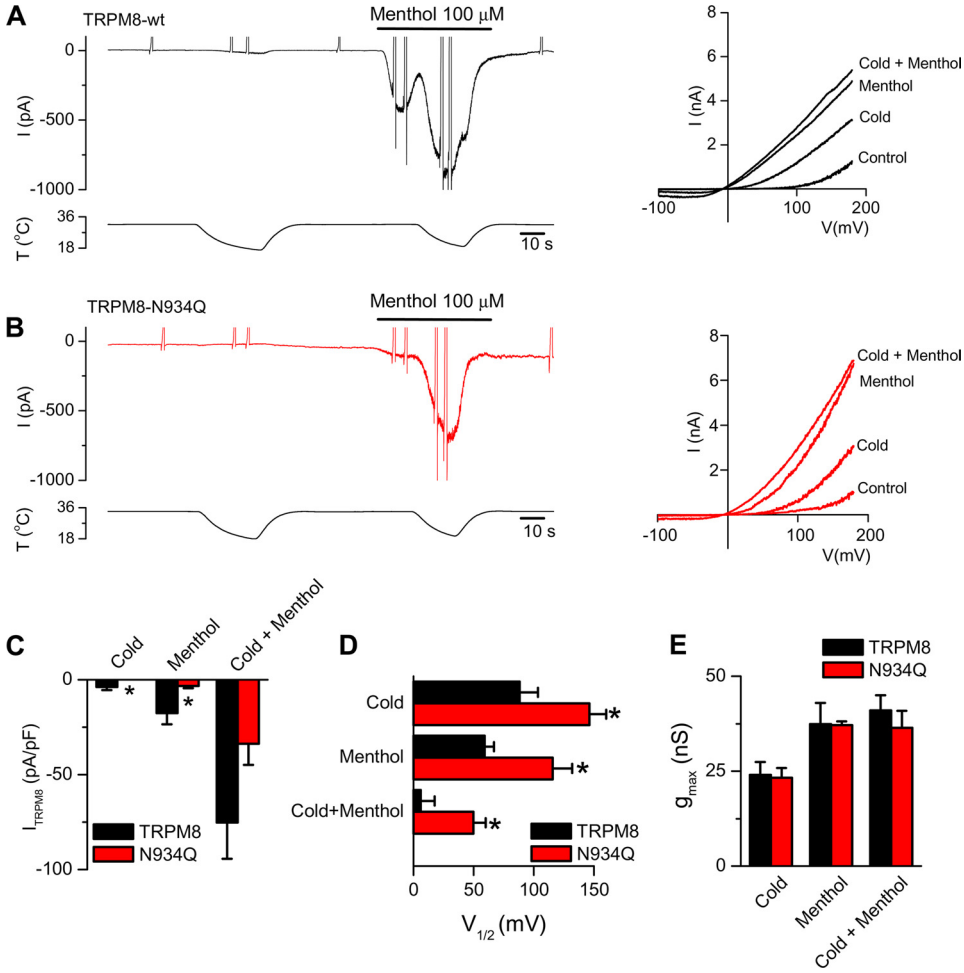

FIGURE 4. **Suppression of *N*-glycosylation causes a shift in the voltage activation of TRPM8 toward more positive potentials.** *A,* whole-cell current recorded at −60 mV in HEK293 cells transfected with TRPM8-WT channels during two consecutive temperature drops and an application of 100 μM menthol. The spike-like currents are the truncated responses to voltage ramps (−100 to +180 mV, 1400 ms duration). *Traces* on the *right* are current-voltage relationship of TRPM8-transfected cells at 33 °C in control solution (*control*), at 20 °C in control solution (*cold*), 100 μM menthol at 33 °C (*menthol*), and during application of 100 μM menthol at 20 °C (*cold plus menthol*). *B,* same experimental protocol as in *A* but on mutated TRPM8-N934Q channels. *C, bar graph* of the mean results obtained in experiments like *A*, showing the maximal current at −60 mV in different conditions (cold, menthol, and cold plus menthol). *D–E,* mean values of $V_{1/2}$ and g_{max} obtained from the fits of the currents to Equation 1. *Black bars* correspond to control and *red bars* to the unglycosylated channel. Statistical significance was assessed with a two-tailed unpaired Student's *t* test: *, $p < 0,05$; $n = 7$ for TRPM8-WT and $n = 8$ for TRPM8-N934Q.

TABLE 1

Summary of the effects of *N*-glycosylation on TRPM8 voltage-dependent activation

Absolute values of the parameter slope, g_{max}, and $V_{½}$ obtained from the fits *I-V* curves obtained from voltage ramps (−100 to +180 mV) to a Boltzmann linear function. The data are given as means ± S.E. To assess statistical significance, unpaired *t* test was performed between the parameters obtained for TRPM8-WT and TRPM8-N934Q channels, in each condition (cold, menthol, and cold plus menthol).

	Cold		Menthol		Cold + menthol	
	TRPM8-WT	TRPM8-N934Q	TRPM8-WT	TRPM8-N934Q	TRPM8-WT	TRPM8-N934Q
G_{max} (nanosiemens)	24.0 ± 3.3	23.3 ± 2.6	37.4 ± 5.5	37.1 ± 3.8	41.0 ± 4.0	36.4 ± 4.5
V_{rev} (mV)	−6.6 ± 3.7	0.0 ± 3.7	−13.5 ± 1.4	−9.9 ± 1.4	−8.2 ± 0.7	−10.6 ± 0.8
$V_{½}$ (mV)	88.3 ± 15.0	146.2 ± 13.9[a]	59.1 ± 7.7	115.8 ± 16.2[a]	5.9 ± 11.6	49.8 ± 10.2[a]
Slope	41.9 ± 2.1	39.3 ± 1.7	52.5 ± 4.9	46.6 ± 2.5	75.1 ± 14.0	53.9 ± 3.1
N	8	7	8	7	8	7

[a] Statistical significance is indicated ($p < 0.05$).

tive trigeminal primary sensory neurons, where the channel is expressed endogenously. We compared the responses to cold and menthol of control and tunicamycin-treated neurons (Fig. 6). As shown in Fig. 6, *A–C*, treatment with tunicamycin caused a significant decrease in the response to cold or menthol stimuli applied alone. In contrast, responses to saturating stimuli (menthol plus cold) do not show significant differences, identical to the observations made in recombinant channels.

In TRPM8-transfected HEK293 cells, the Ca^{2+} entry following a cold or menthol stimulus is determined directly by TRPM8 activity. In contrast, in neurons most of the Ca^{2+} rise detected comes from the activity of voltage-dependent calcium channels, which open during the firing of action potentials following the depolarization produced by the activation of TRPM8. Therefore, inhibition of *N*-glycosylation in neurons could alter the function and/or traffic of other *N*-glycosylated

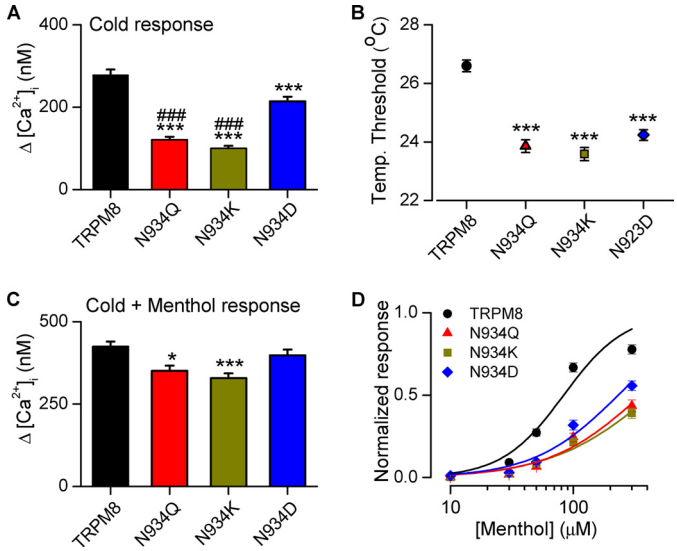

FIGURE 5. **Addition of a negative charge at the position 934 partially recovers the responses to cold and menthol in the unglycosylated TRPM8 mutant.** *A* and *B,* mean values of the $[Ca^{2+}]_i$ response amplitude to cold (*A*), and the temperature threshold (*B*) in wild type channels and in three different mutants. Statistical significance was assessed with a one-way analysis of variance test in combination with Bonferroni post hoc test: ***, $p <$ 0.001 to TRPM8-WT value, and ###, $p < 0.001$ to TRPM8-N934D value. $n = 141$ (TRPM8-WT); $n = 162$ (TRPM8-N934Q); $n = 180$ (TRPM8-N934K); $n = 190$ (TRPM8-N934D). *C,* mean values of the $[Ca^{2+}]_i$ response amplitude to cold plus menthol. Statistical significance was assessed with a one-way analysis of variance test in combination with Bonferroni post hoc test: *, $p < 0.05$; ***, $p <$ 0.001 to TRPM8-WT. $n = 82$ (TRPM8-WT); $n = 60$ (TRPM8-N934Q); $n = 75$ (TRPM8-N934K); $n = 82$ (TRPM8-N934D). *D,* dose-response curves for menthol in WT and different mutant TRPM8 channels expressed in HEK293 cells. The *solid lines* represent fits to Hill equation that yield an EC_{50} 83 ± 13 μM for TRPM8-WT ($n = 82$), 356 ± 13 μM for TRPM8-N934Q ($n = 60$), 437 ± 71 μM for TRPM8-N934K ($n = 75$), and 232 ± 30 μM ($n = 82$) for N934D. For each condition, the response amplitude was normalized to that obtained with a combined pulse of cold and 300 μM menthol (*i.e.* the maximal response).

ion channels, and this change might affect, in an unspecific manner, the neuronal responses to cold and menthol stimuli. To address this question, we also applied a brief pulse of elevated K^+ at the end of the protocol. In this way, we could estimate the number of viable neurons, determine the percentage of cold-sensitive cells, and compare the amplitude of their $[Ca^{2+}]_i$ response to this depolarizing stimulus. The proportion of cold-sensitive neurons was similar for both conditions, 19% ($n = 116$) in control *versus* 16% ($n = 82$) in tunicamycin-treated cultures ($p > 0.05$, *z* test). In the same way, the responses to a high K^+ pulse (*i.e.* depolarizing) did not exhibit significant changes after treatment with tunicamycin; the increment in $[Ca^{2+}]_i$ was 111.7 ± 3.8 nM in control neurons ($n = 116$) and 132.2 ± 5.8 nM after tunicamycin treatment ($n = 82$) ($p > 0.05$, *t* test). These data, together with the fact that responses to saturating stimuli do not change, suggest that *N*-glycosylation of TRPM8 has an important role in the intrinsic activity of native TRPM8 channels.

Finally, we assessed the contribution of *N*-glycosylation to the establishment of the temperature threshold of cold thermoreceptor neurons. Previously, we found that thermal sensitivity of native TRPM8 is shifted to much higher temperatures than channels expressed in recombinant systems (8, 36–39). Here, we confirmed these findings, with a mean cold temperature threshold of 28.4 ± 0.7 °C in neurons compared with 24.7 ± 0.3 °C in transfected HEK293 ($p < 0.001$) (Fig. 6*D*). Remarkably, after tunicamycin treatment, these differences were abolished (22.6 ± 0.7 °C in neurons *versus* 22.7 ± 0.3 °C in HEK293 cells). These results indicate that *N*-glycosylation of TRPM8 has an important role in tuning the temperature threshold of cold sensory neurons.

DISCUSSION

Combining molecular, pharmacological, and electrophysiological approaches, we have characterized the impact of *N*-glycosylation on the activity of thermosensitive TRPM8 channels in recombinant cellular expression systems and in sensory neurons expressing native TRPM8 channels.

Effects of N-Glycosylation on Traffic and Function of TRPM8 Ion Channels—*N*-Glycosylation can modulate the activity of TRP channels by affecting their subcellular localization (TRPV5 (25) and TRPV4 (27)) or changing their biophysical properties (TRPC3 and TRPC6 (26) and TRPV1 (28)). Previous studies on TRPM8 reported that lack of *N*-glycosylation causes a reduction in maximal responses to cold temperature (12) and menthol (13), a finding we could confirm. The authors interpreted these results as a defect in the traffic of unglycosylated channels (*i.e.* TRPM8-N934Q mutant) to the cell surface. However, both groups also suggested the possibility that this post-translational modification could also have a direct effect on TRPM8 biophysical properties. In our hands, using a biotinylation assay, we could not find a significant difference in the surface expression of unglycosylated TRPM8 channels on the plasma membrane. Moreover, electrophysiological recordings of whole-cell currents, including nonstationary variance analysis, also indicate that the number of functional channels at the plasma membrane is similar in cells expressing TRPM8-WT and TRPM8-N934Q channels. Altogether, these results and the evaluation of functional of TRPM8 channels in intracellular compartments using calcium imaging do not support a major defect in traffic. In contrast, analysis of the temperature activation threshold and the menthol dose-response show that the TRPM8-N934Q mutant is significantly less sensitive to thermal and chemical agonists. The fact that responses to both agonists, cold and menthol, are similarly reduced suggests that *N*-glycosylation affects a general mechanism in channel activity. It has been reported that the sensitivity of TRPM8 to cold and menthol is mediated by different effective sites within the channel structure (40, 41). These findings do not preclude the possibility that thermal and chemical activation could be coupled to a third gating mechanism, like voltage (7). Thus, an effect on the gating mechanism could explain the observed deficits in the responses to cold and menthol. Indeed, the electrophysiological analysis revealed that lack of glycosylation leads to a shift in the voltage activation curve of TRPM8 toward more positive potentials, decreasing the probability of the channel to be opened by cold and menthol at physiological membrane potentials, with important implications for their physiological role in native systems (see below).

Role of N-Glycosylation on Biophysical Properties of TRP Channels—The biophysical properties of other TRP channels strongly depend on this kind of post-translational modification. For example, TRPC3 and TRPC6 undergo mono- and di-glyco-

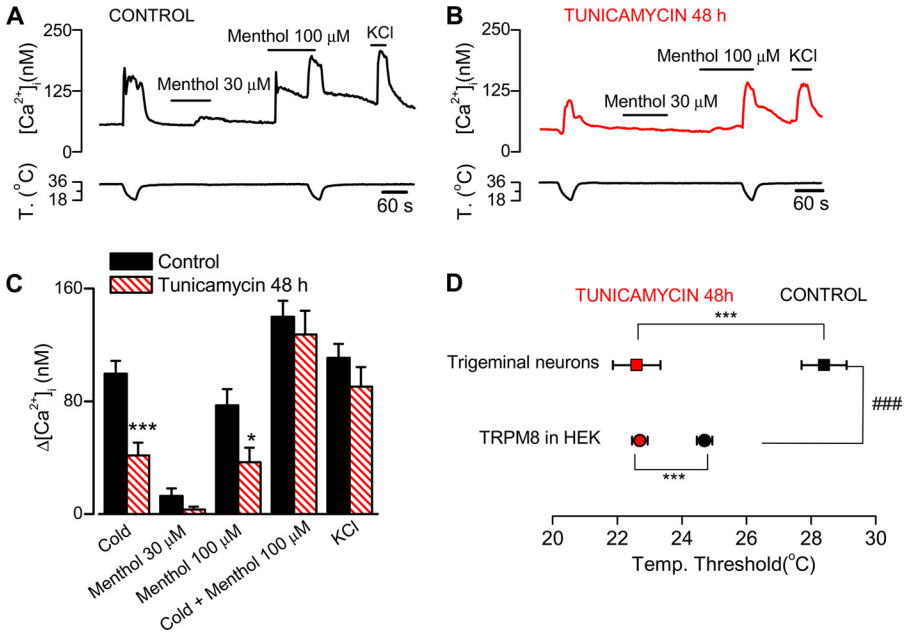

FIGURE 6. ***N*-Glycosylation of TRPM8 has a strong influence on the temperature threshold of cold-sensitive neurons.** *A* and *B*, time course of ratiometric $[Ca^{2+}]_i$ responses in trigeminal cold-sensitive neurons during cooling ramps, applications of menthol at different concentrations and depolarization induced by 30 mM KCl, in control conditions and after 48 h of exposure to tunicamycin (5 μg/ml). *C*, mean evoked $[Ca^{2+}]_i$ responses for the experiments in *A* and *B*. Statistical significance was assessed with a two-tailed unpaired Student's *t* test. *, $p < 0.05$; ***, $p < 0.001$. $n = 22$ (control); $n = 14$ (tunicamycin). *D*, average temperature threshold of cold-sensitive neurons and HEK293 cells transfected with TRPM8-WT, in control condition and after tunicamycin treatment. Statistical significance was assessed with a one-way analysis of variance test in combination with Bonferroni post hoc correction, ***, $p < 0.001$ compared with their control value; ###, $p < 0.001$ comparing trigeminal neurons *versus* transfected human embryonic kidney cells in control conditions. $n = 22$ (TG control); $n = 14$ (TG tunicamycin); $n = 95$ (HEK293-TRPM8 WT, control); $n = 105$ (HEK293-TRPM8 WT, tunicamycin).

sylation, respectively, that modify their function (26). Both channels share an *N*-linked glycosylation site at the first extracellular loop, between transmembrane segments 1 and 2. The TRPC6 channel is also glycosylated at a second site on the second extracellular loop, between transmembrane segments 3 and 4 (26). Elimination of the second glycosylation site in TRPC6, without modification of the *N*-glycosylation site on the first extracellular loop, converts the tightly regulated TRPC6 channel into a constitutively active channel, similar to the TRPC3 phenotype (26). Also worth mentioning, these authors found no differences between wild type and unglycosylated mutants in maximal current densities upon agonist stimulation, similar to our results.

Interestingly, TRPV1 shares with TRPM8 an *N*-linked glycosylation site immediately adjacent to the pore-forming loop, at position 604 (42). A functional study of the unglycosylated TRPV1 channel (TRPV1-N604T) showed that this mutant presents greater sensitivity to the TRPV1 agonist capsaicin than the wild type form and a reduced sensitivity to its competitive inhibitor capsazepine (28). These results suggest that lacking *N*-glycosylation alters gating properties of the channel, but in this case with the opposite effect than that observed in TRPM8.

Our finding that removal of glycosylation produces a rightward (depolarizing) shift in the voltage-dependent activation of TRPM8 is consistent with previous findings in voltage-gated Na^+ and K^+ channels (15, 19, 43). Regarding the mechanism, some studies strongly favor a surface charge effect (44). For example, in voltage-gated Na^+ channels, it has been suggested that negatively charged sialic acid residues, a type of *N*-linked glycan, contribute to the negative surface potential. Reducing channel sialylation produced large alterations in the voltage dependence of channel gating by an electrostatic mechanism (15, 16, 20). However, it has been suggested that sialic acid residues on TRPM8 do not contribute significantly to the negative surface charge sensed by the voltage sensor (45). This result is not incompatible with our findings because it is well established that sialic acid and *N*-glycosylation can have differential effects on channel gating (46). Further studies are needed to establish which mechanisms determine the alteration in gating produced by *N*-glycosylation of TRPM8.

In TRPM8, position 934 is located close to the extracellular end of the transmembrane domain S6, possibly located at the external pore vestibule (47). Previous studies have identified several residues in this microdomain that interact with extracellular cations and mediate functional modulation of TRP channels. These include Glu-543 in the potentiation by La^{3+} and H^+ of TRPC5 (48, 49), Glu-E600 in the modulation of TRPV1 by H^+ (50), and His-896 in the recovery from H^+-enhanced inactivation of TRPM5 (51). In the case of TRPM2 channel, Glu-960 may also directly interact with extracellular Ca^{2+}, and mutations in this position reduce its interaction with this divalent cation (52). In TRPM8, the equivalent position to Glu-960 is Glu-935. Thus, the local negative environment provided by the *N*-glycosylation at position 934 could also affect the Ca^{2+} permeability. In line with this hypothesis, we show that TRPM8-N934D mutant (where the original asparagine is replaced by a negatively charged amino acid) exhibited a partial recovery of the responses to cold and menthol compared with TRPM8-N934Q mutant. Higher permeability to Ca^{2+} of the TRPM8-N934D mutant compared with the TRPM8-N934Q and TRPM8-N934K would explain their potentiated Ca^{2+} responses. Further studies are necessary to clarify this point.

N-Glycosylation of TRPM8 Is a Critical Determinant of Cold Sensitivity of Cold Thermoreceptor Neurons—To determine the physiological relevance of *N*-glycosylation, it is essential to evaluate its impact in native systems. A representative case is TRPV1, which appears as a *N*-glycosylated protein in heterologous systems, whereas in the native system this modification is not detected (24). In contrast, we found that TRPM8 channels are *N*-glycosylated in trigeminal ganglion neurons. Moreover, as in the recombinant system, inhibition of *N*-glycosylation by tunicamycin treatment reduced the responses of the channel to cold and menthol, without affecting the response to saturating or depolarizing stimuli or the percentage of TRPM8-expressing cells. Our observations indicate that treatment with tunicamycin does not compromise the expression of the channel or the excitability of the neuron, suggesting that its effect is mainly due to the role played by *N*-glycosylation on the biophysical properties of TRPM8 channels.

It could be argued that treatment with tunicamycin affects other *N*-glycosylated proteins in sensory neurons, leading to indirect effects on excitability independent of TRPM8. In fact, the lack of *N*-glycosylation in Kv1.1 and Kv1.2 affects the function of these potassium channels (19, 53). These channels are closely related to the establishment of the temperature activation threshold displayed by trigeminal sensory neurons, being the molecular entities underlying the current I_{KD}, which acts as an excitability brake in cold thermoreceptor neurons (29, 38). Specifically, the absence of *N*-glycosylation of Kv1 channels caused a net decrease in its activity (19, 53). Thus, application of tunicamycin should negatively affect I_{KD}, causing an increase in excitability. However, we observed the opposite effect, a net decrease in excitability after tunicamycin treatment, suggesting a larger functional effect on TRPM8 channels compared with Kv1 channels.

An important question still unsolved in the study of the physiology of cold thermoreceptors is why TRPM8 channels expressed in heterologous systems display a shift in their response to lower temperatures compared with channels in the native system. Unglycosylation of native TRPM8 modified the thermal sensitivity of cold thermoreceptor neurons dramatically, shifting the mean threshold to around 6 °C to lower temperatures, in contrast with the 2 °C shift reported in the recombinant system. Our results show the importance of *N*-glycosylation in the physiological function of the TRPM8 channel and suggest that in native systems this post-translational modification shifts the operating range of TRPM8 to higher temperatures. We propose that this post-translational modification is a critical molecular determinant in the establishment of cold sensitivity in primary sensory neurons. This result is also relevant for current efforts, trying to design novel thermogenetic tools for *in vivo* probing of neuronal circuits. Scientists building these technologies (54) should be aware that the thermal activation threshold of a TRP channel *in vivo* may be quite different from the threshold reported *in vitro*.

In recombinant systems, the overexpression of TRPM8 may saturate the *N*-glycosylation machinery, resulting in the incomplete processing of the channel at the cell surface, resulting in a channel that is less sensitive to agonists. One example of this phenomenon is observed in Fig. 1*A* as follows: trigeminal neurons lack the nonglycosylated form of TRPM8 (the lower band observed in Western blots from recombinant channels expressed in HEK293 cells). In addition, in Fig. 1*F*, the wild type TRPM8 from the plasma membrane fraction clearly shows the bands corresponding to the fully processed and immature forms of the channel. Moreover, the composition of *N*-glycosylation may also vary depending on the cellular context in which this post-translational modification occurs (55), thus having an influence on the function of the channel.

We also have to consider the general role of *N*-glycosylation in the proper targeting of the protein to its functional compartment. In a previous report, we showed that segregation of TRPM8 in lipid rafts is favored by glycosylation at asparagine 934 (14). Our results indicated that TRPM8 could be affected by the lipid environment, showing that menthol- and cold-mediated responses of TRPM8 are potentiated when the association of the channel with lipid rafts is prevented (14). In this scenario, unglycosylated channels, which show an important reduction in the association to lipid raft (14), should display higher responses to agonists than TRPM8-WT channel. The results presented here showed that the nonglycosylated mutant has a reduced response to cold and menthol stimuli, indicating that *N*-glycosylation *per se*, independent of the lipid raft association, has an important role in gating properties of the channel. However, we cannot exclude that correct targeting of TRPM8 in sensory neurons mediated by *N*-glycosylation could affect protein-protein interactions that could modulate channel properties such as their temperature activation threshold.

In conclusion, in this report we show that unglycosylation of TRPM8 affects its biophysical properties, shifting the voltage activation curve toward more positive potentials and leading to a marked reduction in the response to canonical activators of the channel. The reduction in activity can be overcome by supramaximal stimuli, suggesting that defects in the traffic of channels to the plasma membrane are not the main determinant of the reduced response. Finally, our results suggest that *N*-glycosylation of TRPM8 could play an important modulatory role in sensory neurons, contributing to the setting of the temperature sensitivity of cold thermoreceptor terminals.

Acknowledgments—We thank Annika Mälkiä and María José López for helpful advice and comments to the manuscript and Eva Quintero, the late Alfonso Pérez, Ana Miralles, and Sophie Sarret for excellent technical assistance.

REFERENCES

1. Hensel, H. (1981) Thermoreception and temperature regulation. *Monogr. Physiol. Soc.* **38,** 1–321
2. Dhaka, A., Viswanath, V., and Patapoutian, A. (2006) Trp ion channels and temperature sensation. *Annu. Rev. Neurosci.* **29,** 135–161
3. McKemy, D. D. (2005) How cold is it? TRPM8 and TRPA1 in the molecular logic of cold sensation. *Mol. Pain* **1,** 16
4. McKemy, D. D., Neuhausser, W. M., and Julius, D. (2002) Identification of a cold receptor reveals a general role for TRP channels in thermosensation. *Nature* **416,** 52–58
5. Peier, A. M., Moqrich, A., Hergarden, A. C., Reeve, A. J., Andersson, D. A., Story, G. M., Earley, T. J., Dragoni, I., McIntyre, P., Bevan, S., and Patapoutian, A. (2002) A TRP channel that senses cold stimuli and menthol. *Cell* **108,** 705–715

6. Brauchi, S., Orio, P., and Latorre, R. (2004) Clues to understanding cold sensation. Thermodynamics and electrophysiological analysis of the cold receptor TRPM8. *Proc. Natl. Acad. Sci. U.S.A.* **101,** 15494–15499
7. Voets, T., Droogmans, G., Wissenbach, U., Janssens, A., Flockerzi, V., and Nilius, B. (2004) The principle of temperature-dependent gating in cold- and heat-sensitive TRP channels. *Nature* **430,** 748–754
8. Mälkiä, A., Madrid, R., Meseguer, V., de la Peña, E., Valero, M., Belmonte, C., and Viana, F. (2007) Bidirectional shifts of TRPM8 channel gating by temperature and chemical agents modulate the cold sensitivity of mammalian thermoreceptors. *J. Physiol.* **581,** 155–174
9. Bautista, D. M., Siemens, J., Glazer, J. M., Tsuruda, P. R., Basbaum, A. I., Stucky, C. L., Jordt, S. E., and Julius, D. (2007) The menthol receptor TRPM8 is the principal detector of environmental cold. *Nature* **448,** 204–208
10. Colburn, R. W., Lubin, M. L., Stone, D. J., Jr., Wang, Y., Lawrence, D., D'Andrea, M. R., Brandt, M. R., Liu, Y., Flores, C. M., and Qin, N. (2007) Attenuated cold sensitivity in TRPM8 null mice. *Neuron* **54,** 379–386
11. Dhaka, A., Murray, A. N., Mathur, J., Earley, T. J., Petrus, M. J., and Patapoutian, A. (2007) TRPM8 is required for cold sensation in mice. *Neuron* **54,** 371–378
12. Dragoni, I., Guida, E., and McIntyre, P. (2006) The cold and menthol receptor TRPM8 contains a functionally important double cysteine motif. *J. Biol. Chem.* **281,** 37353–37360
13. Erler, I., Al-Ansary, D. M., Wissenbach, U., Wagner, T. F., Flockerzi, V., and Niemeyer, B. A. (2006) Trafficking and assembly of the cold-sensitive TRPM8 channel. *J. Biol. Chem.* **281,** 38396–38404
14. Morenilla-Palao, C., Pertusa, M., Meseguer, V., Cabedo, H., and Viana, F. (2009) Lipid raft segregation modulates TRPM8 channel activity. *J. Biol. Chem.* **284,** 9215–9224
15. Bennett, E., Urcan, M. S., Tinkle, S. S., Koszowski, A. G., and Levinson, S. R. (1997) Contribution of sialic acid to the voltage dependence of sodium channel gating. A possible electrostatic mechanism. *J. Gen. Physiol.* **109,** 327–343
16. Recio-Pinto, E., Thornhill, W. B., Duch, D. S., Levinson, S. R., and Urban, B. W. (1990) Neuraminidase treatment modifies the function of electroplax sodium channels in planar lipid bilayers. *Neuron* **5,** 675–684
17. Rho, S., Lee, H. M., Lee, K., and Park, C. (2000) Effects of mutation at a conserved *N*-glycosylation site in the bovine retinal cyclic nucleotide-gated ion channel. *FEBS Lett.* **478,** 246–252
18. Ufret-Vincenty, C. A., Baro, D. J., Lederer, W. J., Rockman, H. A., Quinones, L. E., and Santana, L. F. (2001) Role of sodium channel deglycosylation in the genesis of cardiac arrhythmias in heart failure. *J. Biol. Chem.* **276,** 28197–28203
19. Watanabe, I., Wang, H. G., Sutachan, J. J., Zhu, J., Recio-Pinto, E., and Thornhill, W. B. (2003) Glycosylation affects rat Kv1.1 potassium channel gating by a combined surface potential and cooperative subunit interaction mechanism. *J. Physiol.* **550,** 51–66
20. Zhang, Y., Hartmann, H. A., and Satin, J. (1999) Glycosylation influences voltage-dependent gating of cardiac and skeletal muscle sodium channels. *J. Membr. Biol.* **171,** 195–207
21. Tyrrell, L., Renganathan, M., Dib-Hajj, S. D., and Waxman, S. G. (2001) Glycosylation alters steady-state inactivation of sodium channel Nav1.9/NaN in dorsal root ganglion neurons and is developmentally regulated. *J. Neurosci.* **21,** 9629–9637
22. Cohen, D. M. (2006) Regulation of TRP channels by *N*-linked glycosylation. *Semin. Cell Dev. Biol.* **17,** 630–637
23. Vannier, B., Zhu, X., Brown, D., and Birnbaumer, L. (1998) The membrane topology of human transient receptor potential 3 as inferred from glycosylation-scanning mutagenesis and epitope immunocytochemistry. *J. Biol. Chem.* **273,** 8675–8679
24. Kedei, N., Szabo, T., Lile, J. D., Treanor, J. J., Olah, Z., Iadarola, M. J., and Blumberg, P. M. (2001) Analysis of the native quaternary structure of vanilloid receptor 1. *J. Biol. Chem.* **276,** 28613–28619
25. Chang, Q., Hoefs, S., van der Kemp, A. W., Topala, C. N., Bindels, R. J., and Hoenderop, J. G. (2005) The β-glucuronidase klotho hydrolyzes and activates the TRPV5 channel. *Science* **310,** 490–493
26. Dietrich, A., Mederos y Schnitzler, M., Emmel, J., Kalwa, H., Hofmann, T., and Gudermann, T. (2003) *N*-Linked protein glycosylation is a major determinant for basal TRPC3 and TRPC6 channel activity. *J. Biol. Chem.* **278,** 47842–47852
27. Xu, H., Fu, Y., Tian, W., and Cohen, D. M. (2006) Glycosylation of the osmoresponsive transient receptor potential channel TRPV4 on Asn-651 influences membrane trafficking. *Am. J. Physiol. Renal Physiol.* **290,** F1103–F1109
28. Wirkner, K., Hognestad, H., Jahnel, R., Hucho, F., and Illes, P. (2005) Characterization of rat transient receptor potential vanilloid 1 receptors lacking the *N*-glycosylation site N604. *Neuroreport* **16,** 997–1001
29. Viana, F., de la Peña, E., and Belmonte, C. (2002) Specificity of cold thermotransduction is determined by differential ionic channel expression. *Nat. Neurosci.* **5,** 254–260
30. Mahoney, W. C., and Duksin, D. (1979) Biological activities of the two major components of tunicamycin. *J. Biol. Chem.* **254,** 6572–6576
31. Klausner, R. D., Donaldson, J. G., and Lippincott-Schwartz, J. (1992) Brefeldin A. Insights into the control of membrane traffic and organelle structure. *J. Cell Biol.* **116,** 1071–1080
32. Varki, A., Cummings, R., Esko, J., Freeze, H., Hart, G., and Marth, J. (1999) *Essentials of Glycobiology*, Cold Spring Harbor Laboratory Press, Cold Spring Harbor, NY
33. Valero, M., Morenilla-Palao, C., Belmonte, C., and Viana, F. (2011) Pharmacological and functional properties of TRPM8 channels in prostate tumor cells. *Pflugers Arch.* **461,** 99–114
34. Tsuzuki, K., Xing, H., Ling, J., and Gu, J. G. (2004) Menthol-induced Ca^{2+} release from presynaptic Ca^{2+} stores potentiates sensory synaptic transmission. *J. Neurosci.* **24,** 762–771
35. Alvarez, O., Gonzalez, C., and Latorre, R. (2002) Counting channels. A tutorial guide on ion channel fluctuation analysis. *Adv. Physiol. Educ.* **26,** 327–341
36. de la Peña, E., Mälkiä, A., Cabedo, H., Belmonte, C., and Viana, F. (2005) The contribution of TRPM8 channels to cold sensing in mammalian neurones. *J. Physiol.* **567,** 415–426
37. Madrid, R., Donovan-Rodríguez, T., Meseguer, V., Acosta, M. C., Belmonte, C., and Viana, F. (2006) Contribution of TRPM8 channels to cold transduction in primary sensory neurons and peripheral nerve terminals. *J. Neurosci.* **26,** 12512–12525
38. Madrid, R., de la Peña, E., Donovan-Rodriguez, T., Belmonte, C., and Viana, F. (2009) Variable threshold of trigeminal cold-thermosensitive neurons is determined by a balance between TRPM8 and Kv1 potassium channels. *J. Neurosci.* **29,** 3120–3131
39. Parra, A., Madrid, R., Echevarria, D., del Olmo S., Morenilla-Palao, C., Acosta, M. C., Gallar, J., Dhaka, A., Viana, F., and Belmonte, C. (2010) Ocular surface wetness is regulated by TRPM8-dependent cold thermoreceptors of the cornea. *Nat. Med.* **16,** 1396–1399
40. Bandell, M., Dubin, A. E., Petrus, M. J., Orth, A., Mathur, J., Hwang, S. W., and Patapoutian, A. (2006) High throughput random mutagenesis screen reveals TRPM8 residues specifically required for activation by menthol. *Nat. Neurosci.* **9,** 493–500
41. Brauchi, S., Orta, G., Salazar, M., Rosenmann, E., and Latorre, R. (2006) A hot-sensing cold receptor. C-terminal domain determines thermosensation in transient receptor potential channels. *J. Neurosci.* **26,** 4835–4840
42. Jahnel, R., Dreger, M., Gillen, C., Bender, O., Kurreck, J., and Hucho, F. (2001) Biochemical characterization of the vanilloid receptor 1 expressed in a dorsal root ganglia derived cell line. *Eur. J. Biochem.* **268,** 5489–5496
43. Freeman, L. C., Lippold, J. J., and Mitchell, K. E. (2000) Glycosylation influences gating and pH sensitivity of I(sK). *J. Membr. Biol.* **177,** 65–79
44. Hille, B., Woodhull, A. M., and Shapiro, B. I. (1975) Negative surface charge near sodium channels of nerve. Divalent ions, monovalent ions, and pH. *Philos. Trans. R. Soc. Lond. B Biol. Sci.* **270,** 301–318
45. Mahieu, F., Janssens, A., Gees, M., Talavera, K., Nilius, B., and Voets, T. (2010) Modulation of the cold-activated cation channel TRPM8 by surface charge screening. *J. Physiol.* **588,** 315–324
46. Johnson, D., and Bennett, E. S. (2008) Gating of the shaker potassium channel is modulated differentially by *N*-glycosylation and sialic acids. *Pflugers Arch.* **456,** 393–405
47. Owsianik, G., Talavera, K., Voets, T., and Nilius, B. (2006) Permeation and selectivity of TRP channels. *Annu. Rev. Physiol.* **68,** 685–717
48. Jung, S., Mühle, A., Schaefer, M., Strotmann, R., Schultz, G., and Plant,

T. D. (2003) Lanthanides potentiate TRPC5 currents by an action at extracellular sites close to the pore mouth. *J. Biol. Chem.* **278,** 3562–3571
49. Semtner, M., Schaefer, M., Pinkenburg, O., and Plant, T. D. (2007) Potentiation of TRPC5 by protons. *J. Biol. Chem.* **282,** 33868–33878
50. Jordt, S. E., Tominaga, M., and Julius, D. (2000) Acid potentiation of the capsaicin receptor determined by a key extracellular site. *Proc. Natl. Acad. Sci. U.S.A.* **97,** 8134–8139
51. Liu, D., Zhang, Z., and Liman, E. R. (2005) Extracellular acid block and acid-enhanced inactivation of the Ca^{2+}-activated cation channel TRPM5 involve residues in the S3-S4 and S5-S6 extracellular domains. *J. Biol. Chem.* **280,** 20691–20699
52. Xia, R., Mei, Z. Z., Mao, H. J., Yang, W., Dong, L., Bradley, H., Beech, D. J., and Jiang, L. H. (2008) Identification of pore residues engaged in determining divalent cationic permeation in transient receptor potential melastatin subtype channel 2. *J. Biol. Chem.* **283,** 27426–27432
53. Thornhill, W. B., Wu, M. B., Jiang, X., Wu, X., Morgan, P. T., and Margiotta, J. F. (1996) Expression of Kv1.1 delayed rectifier potassium channels in Lec mutant Chinese hamster ovary cell lines reveals a role for sialidation in channel function. *J. Biol. Chem.* **271,** 19093–19098
54. Bernstein, J. G., Garrity, P. A., and Boyden, E. S. (2012) Optogenetics and thermogenetics. Technologies for controlling the activity of targeted cells within intact neural circuits. *Curr. Opin. Neurobiol.* **22,** 61–71
55. Hsieh, P., Rosner, M. R., and Robbins, P. W. (1983) Host-dependent variation of asparagine-linked oligosaccharides at individual glycosylation sites of Sindbis virus glycoproteins. *J. Biol. Chem.* **258,** 2548–2554
56. Nilius, B., Mahieu, F., Prenen, J., Janssens, A., Owsianik, G., Vennekens, R., and Voets, T. (2006) The Ca^{2+}-activated cation channel TRPM4 is regulated by phosphatidylinositol 4,5-biphosphate. *EMBO J.* **25,** 467–478